

See discussions, stats, and author profiles for this publication at: <https://www.researchgate.net/publication/230324162>

# Formation of Human Telomeric G-quadruplex Structures Induced by the Quaternary Benzophenanthridine Alkaloids: Sanguinarine, Nitidine, and Chelerythrine

ARTICLE *in* CHINESE JOURNAL OF CHEMISTRY · MAY 2010

Impact Factor: 1.58 · DOI: 10.1002/cjoc.201090145

CITATIONS

7

READS

28

8 AUTHORS, INCLUDING:



**Jun-Feng Xiang**

Chinese Academy of Sciences

185 PUBLICATIONS 2,873 CITATIONS

SEE PROFILE



**Qianfan Yang**

Chinese Academy of Sciences

34 PUBLICATIONS 335 CITATIONS

SEE PROFILE



**Qiuju Zhou**

Université de Mons

21 PUBLICATIONS 285 CITATIONS

SEE PROFILE



**Zhang Xiufeng**

Tsinghua University

19 PUBLICATIONS 189 CITATIONS

SEE PROFILE

# Formation of Human Telomeric G-quadruplex Structures Induced by the Quaternary Benzophenanthridine Alkaloids: Sanguinarine, Nitidine, and Chelerythrine

Yang, Shu<sup>a,b</sup>(杨舒)    Xiang, Junfeng<sup>\*a</sup>(向俊锋)    Yang, Qianfan<sup>a,b</sup>(杨千帆)  
 Li, Qian<sup>a,b</sup>(李骞)    Zhou, Qiuju<sup>a,b</sup>(周秋菊)    Zhang, Xiufeng<sup>a</sup>(张秀凤)  
 Tang, Yalin<sup>\*a</sup>(唐亚林)    Xu, Guangzhi<sup>a</sup>(徐广智)

<sup>a</sup> Beijing National Laboratory for Molecular Sciences (BNLMS), Centre for Molecular Sciences, State Key Laboratory for Structural Chemistry for Unstable and Stable Species, Institute of Chemistry, Chinese Academy of Sciences (ICCAS), Beijing 100190, China

<sup>b</sup> Graduate University of Chinese Academy of Sciences, Beijing 100049, China

The ligands which can facilitate the formation and stabilize G-quadruplex structures have attracted enormous attention due to their potential ability of inhibiting the telomerase activity and halting tumor cell proliferation. It is noteworthy that the abilities of the quaternary benzophenanthridine alkaloids (QBAs), the very important G-quadruplex binders, in inducing the formation of human telomeric DNA G-quadruplex structures, have not been reported. Herein, the interaction between single-strand human telomeric DNA and three QBAs: Sanguinarine (San), Nitidine (Nit) and Chelerythrine (Che), has been investigated. Although these molecules are very similar in structure, they exhibit significantly different abilities in inducing oligonucleotide d(TTAGGG)<sub>4</sub> (HT4) to specific G-quadruplex structures. Our experimental results indicated that the best ligand San could convert HT4 into anti-parallel G-quadruplex structure completely, followed by Nit, which could transform to mixed-type or hybrid G-quadruplex structure partially, whereas Che could only transform to antiparallel G-quadruplex structure in small quantities. The relative QBAs' inducing abilities as indicated by the CD data are in the order of San > Nit > Che. Further investigation revealed that the G-quadruplex structures from HT4 induced by QBAs are of intramolecular motif. And only sequences with certain length could be induced by QBAs because of their positive charges which could not attract short chain DNA molecules to close to each other and form intermolecular G-quadruplex. In addition, the factors that affect the interaction between HT4 and QBAs were discussed. It is proposed that the thickness of the molecular frame and the steric hindrance are the primary reasons why the subtle differences in QBAs' structure lead to their remarkable differences in inducing the formation of the G-quadruplex structures.

**Keywords** human telomeric DNA, G-quadruplexes, Sanguinarine, Nitidine, Chelerythrine, Alkaloids

## Introduction

Human telomeres, composed of tandem (TTAGGG)<sub>n</sub> repeated DNA sequences with a guanine (G)-rich strand forming a protruding 3' single-strand overhang, have been found at the extremities of eukaryotic chromosomes.<sup>1</sup> They protect the ends of chromosomes from base pair loss and end-to-end fusions encountered in chromosome replication events.<sup>2</sup> The unique mode of telomeric replication depends on telomerase, which is not active in somatic cells but shows elevated levels of expression in 85%–90% of cancerous cells.<sup>3</sup> The 3' G-rich single-strand overhang of human telomere could fold into a tetra-stranded DNA structure (G-quadruplex), where four guanine bases are held in the same plane by a Hoogsteen hydrogen bond array.<sup>4</sup> G-quadruplex structures have been shown to inhibit telomerase activ-

ity.<sup>5</sup> As a result, the ligands with the ability of facilitating the formation or stabilization of G-quadruplex structure have attracted more and more attention as a new class of potentially selective antitumor drugs.<sup>4,6–8</sup>

Since Zahler and his co-workers<sup>5</sup> firstly reported that K<sup>+</sup>-stabilized G-quadruplex structures were able to inhibit telomerase, several groups have devoted themselves to searching G-quadruplex ligands. Although most researches were focused on the ligands which could stabilize the formed G-quadruplex structures, the ligands which could induce the formation of G-quadruplex structures in the absence of cations should not be neglected because some effective anticancer agents were found to exhibit this ability.<sup>9,10</sup>

The quaternary benzophenanthridine alkaloids (QBAs), Sanguinarine (San), Nitidine (Nit), and Chelerythrine (Che) (Figure 1), has been reported to exhibit

\* E-mail: tangyl@iccas.ac.cn, jfxiang@iccas.ac.cn; Fax: 0086-010-6252-2090; Tel.: 0086-010-62522090  
 Received September 18, 2009; revised October 16, 2009; accepted November 23, 2009.

pronounced cytotoxicity<sup>11,12</sup> and anticancer activity,<sup>13</sup> as well as DNA-binding activity and distinct sequence selectivity to double-stranded DNA which was proposed to be one of the molecular mechanisms of its anticancer activity.<sup>14,15</sup> They also possess the characteristics of most effective G-quadruplex ligands, a large electron deficient  $\pi$ -aromatic surface and a positively charged centre<sup>16,17</sup> and San has been reported as a G-quadruplex binder.<sup>18</sup> However, there is no report concerned with their abilities in inducing the formation of human telomeric DNA G-quadruplex structures although such feature may be related with their antitumor activities.

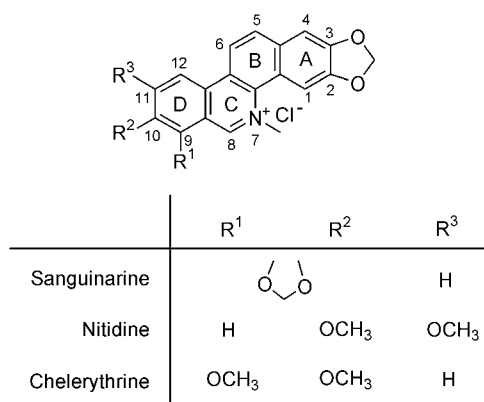


**Figure 1** The structural formulae of three QBAs.

In this paper, these molecules are found to be capable to induce single-strand human telomeric DNA to form G-quadruplex structure. What interests us is that these molecules with very similar structure exhibit different abilities in inducing single-strand DNA to form G-quadruplex structures. Additionally, the reason why the subtle differences in QBAs' structure lead to their remarkable differences in inducing the formation of the G-quadruplex structures is also discussed. This result may help to guide the further finding and designing of the anticancer drugs derived from alkaloids.

## Experimental

### Materials

San, Nit and Che (purity 98%, respectively) (abbreviated as QBAs) were purchased from AR Bio-Tech. Co., Ltd. and used without further purification. All DNA oligonucleotides (Table 1) were obtained from Invitrogen (Beijing, China), purified by PAGE (purity 98%) and used without further purification. Tris and

EDTA were of all analytical reagent grades, purchased from Beijing Chem. Co.

### Sample preparation

The stock solutions of QBAs were prepared by dissolving San, Nit, and Che in Tris-HCl buffer solution (10 mmol·L<sup>-1</sup> Tris-HCl, 1 mmol·L<sup>-1</sup> EDTA, pH 7.4), respectively. The stock solutions of DNA oligonucleotides were prepared by dissolving DNA oligonucleotides in Tris-HCl buffer solution (10 mmol·L<sup>-1</sup> Tris-HCl, 1 mmol·L<sup>-1</sup> EDTA, pH 7.4).

### CD spectroscopy and CD melting experiments

The CD data were collected on a Jasco-J 815 spectropolarimeter. A quartz cell of 1 cm optical path length was used for measurements. The final spectra were the averages of three repetitions. Each spectrum was baseline-corrected and the signal contributions of the Tris-HCl buffer solution were subtracted. The temperature of the cell holder was regulated by a JASCO PTC-423S temperature controller, and the cuvette-holding chamber was flushed with a constant stream of dry N<sub>2</sub> gas to avoid water condensation on the cuvette exterior. Melting curves of the parallel G-quadruplexes were obtained by recording the CD intensity at 292 nm. The heating rate was 1.0 °C·min<sup>-1</sup>.

The samples were prepared by mixing a quantity of QBA stock solution with DNA oligonucleotide stock solution in Tris-HCl buffer solution (10 mmol·L<sup>-1</sup> Tris-HCl, 1 mmol·L<sup>-1</sup> EDTA, pH 7.4). The sample solutions were kept overnight at room temperature before measurement in order to realize the full reaction.

### <sup>1</sup>D NMR

NMR experiments were performed on a Bruker AVANCE 600 spectrometer equipped with a 5 mm BBI probe capable of delivering z-field gradients and TOPSPIN software (Bruker, version 2.0). All experiments were carried out at 298.2 K. The 1D proton spectra were recorded by the standard pulse program p3919gp that applies 3-9-19 pulses with gradients for water suppression.

### ESI-MS

ESI-MS spectra were obtained in the negative-ion mode by using a LCMS-2010A mass spectrometer (Shimadzu). The oligonucleotide solutions were infused directly into the ion source at a flow rate of 70 µL/min. The electrospray source conditions were: 4.5 kV spray voltage, 250 °C capillary temperature. Data were collected and analyzed by using LCMS solution ver3 software developed by Shimadzu, and ten scans were averaged for each spectrum.

### Molecular modeling calculation

The QBA structures were built up on a SGI workstation by using Discovery module of Insight II 2005 software, and the potential of QBAs were assigned to

**Table 1** The naming conventions of the DNAs

DNA oligonucleotides	Abbreviation
d(TTAGGGT)	H7
d(TTAGGGTTAGGG)	HT2
d(AGGGTTAGGGTTAGGGTTAGGG)	H22
d(TTAGGGTTAGGGTTAGGGTTAGGG)	HT4
d(TTGGGTTAGGGTTAGGGTTAGGGA)	H24A

the ESFF force field. Each molecule was fully energy-minimized with 5000 steps of steepest descent (SD) and then 5000 steps of conjugate gradient (CONJ).

## Results and Discussion

### QBAs have abilities to induce HT4 forming distinct G-quadruplexes

CD measurement has been extensively applied to study secondary structures of DNA.<sup>19–21</sup> Different DNA structures give rise to distinct CD spectral features,<sup>22</sup> which help to recognize different DNA motifs conveniently.

HT4, generally presents unfolded motif under salt-deficiency condition, exhibited typical CD signals in 10 mmol·L<sup>−1</sup> Tris-HCl buffer solution (pH 7.4). As shown in Figure 2, addition of San led to distinct changes of the CD spectra: the CD signals of single-strand HT4 decreased and eventually disappeared, while two new CD signals (a positive one at 288 nm and a negative one at 261.5 nm) assigned to antiparallel G-quadruplex structure appeared.<sup>22</sup> In the case of Che, addition of Che led to the appearance of very similar but much weaker spectral changes: the CD signal intensity of single-strand HT4 decreased but the signal did not completely disappear, while two new CD signals (a positive one at 287 nm and a negative one at 253.5 nm) appeared. However, compared with those of San and Che, addition of Nit led to quite different spectral changes: the CD signal intensities assigned to single-strand HT4 decreased while two new positive signals were induced at 271 and 298 nm, respectively, suggesting the formation of a mixed-type or hybrid G-quadruplex structure. Additionally, the remaining shoulder peak at 256 nm indicates small amount of single-strand HT4 remains unchanged.

Proton NMR spectroscopy has been widely used to study the interaction between small molecule ligands and G-quadruplexes.<sup>21</sup> In order to further confirm the formation of distinct G-quadruplex structures induced by QBAs, <sup>1</sup>D NMR spectra of HT4 with QBAs were also investigated. As shown in supporting information, in the absence of K<sup>+</sup> or Na<sup>+</sup>, HT4 is in the form of random single strand and there is no guanine imino proton signal in the downfield region (about  $\delta$  10–12). Addition of San or Nit led to appearance of some obvious imino proton signals assigned to G-quadruplex, which indicates that San and Nit indeed have the ability to induce HT4 from single strand to specific G-quadruplex structure. However, probably because of small interaction force between HT4 and Che, no obvious imino proton signal was induced in the presence of Che (data not shown).

All results suggested that although these three QBA molecules have very similar structures, they exhibit strongly distinct abilities in inducing the formation of G-quadruplex structures.

To clarify the QBAs' different inducing abilities, the

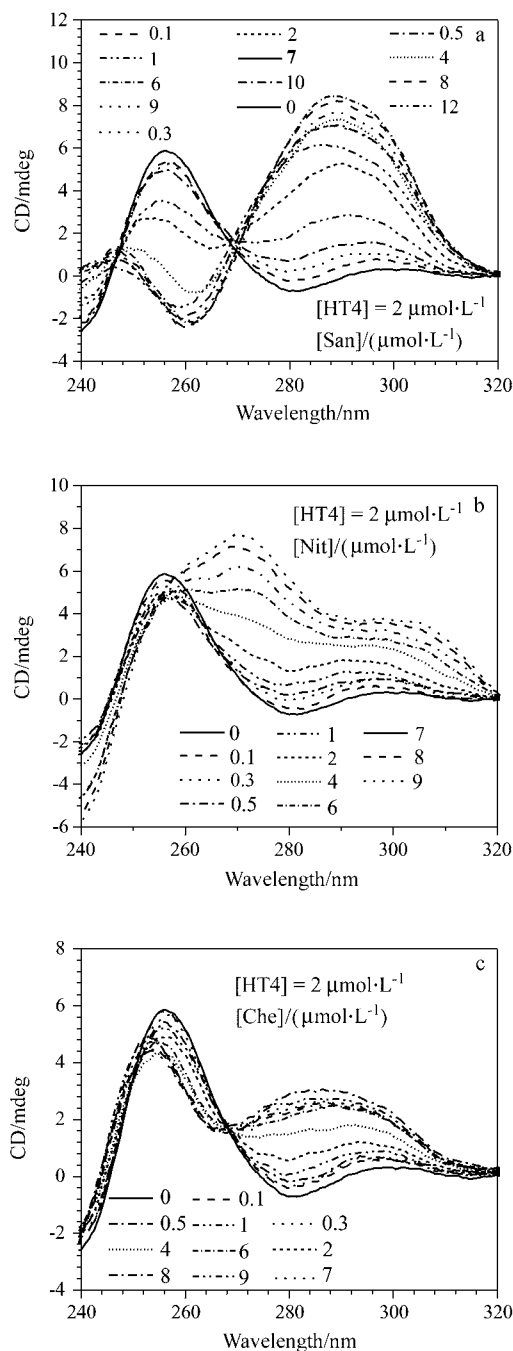


**Figure 2** The CD spectra of 2 μmol·L<sup>−1</sup> HT4 and 2 μmol·L<sup>−1</sup> HT4 with difference concentrations of San (a), Nit (b) and Che (c), respectively.

CD signals assigned to induced antiparallel G-quadruplexes were also analyzed. As shown in Figure 3, the CD signal around 290 nm increased linearly with the ratio [QBAs] : [HT4], and stopped increasing when reaching a limit. The slope of the linear curves at earlier stage in the case of San and Che were highest and lowest, respectively, and that of Nit was middle. According to the method suggested by Walwick and coworkers,<sup>23</sup> the Job curves [dashed lines in Figure 3] of San, Nit and Che intercrossed at about 3.5, 4.2 and 5.7, respectively, indicating the relative QBAs' inducing abilities are in

the order of San > Nit > Che.

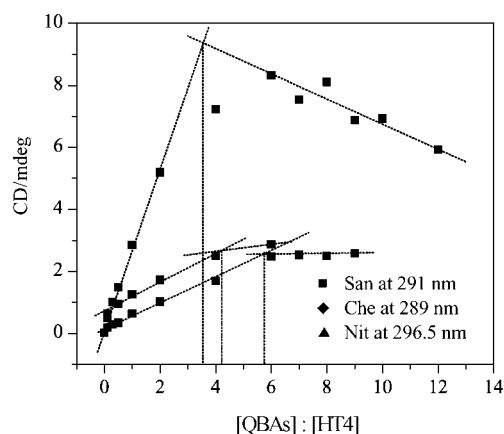


**Figure 3** The changes of  $2 \mu\text{mol}\cdot\text{L}^{-1}$  HT4 CD signals around 290 nm against the ratio of [QBAs] : [HT4].

### Stability of HT4 G-quadruplexes induced by QBAs

In order to discuss the abilities of QBAs inducing HT4 to form specific G-quadruplexes, the stabilities of the induced G-quadruplex structures had been studied.

We applied circular dichroism to monitor the melting temperature ( $T_m$ ) of induced G-quadruplexes at 292 nm (the detailed CD spectra were shown in supporting information). The change of  $T_m$  in the folded and unfolded quadruplex structures upon interacting with ligand provides evidence of thermal stabilization of DNA structure. As shown in Figure 4, the  $T_m$  of HT4 in the presence of  $10 \text{ mmol}\cdot\text{L}^{-1} \text{Na}^+$  is about  $30^\circ\text{C}$ , which is considered as an antiparallel G-quadruplex structure.<sup>22</sup> The  $T_m$  of G-quadruplex induced by San, Nit and Che are about  $42$ ,  $40$  and  $34^\circ\text{C}$ , respectively, which are higher than that of HT4 with  $\text{Na}^+$ , indicating that the HT4-QBAs complexes are more stable than HT4 G-quadruplex induced by cations. Based on the results, it is inferred that the relative interaction forces between HT4 and QBAs are in the order of San > Nit > Che, which is in accordance with their inducing abilities.

### QBAs induce HT4 forming intramolecular G-quadruplexes

Although the CD data have shown that G-quadruplex structure of HT4 is, respectively, formed in the presence of three QBAs, it is not clear which kind of structure is formed, intramolecular or intermolecular. In order to clarify this point, ESI-MS experiments which could identify the formation of intramolecular or intermolecular G-quadruplex based on molecular weight<sup>24,25</sup> were performed. As shown in Figure 5, the peaks signed by ★ are assigned to HT4 and the ones signed by ▲ are assigned to HT4-QBA complex. In the absence of QBAs, the charge of the species at the  $m/z$  ratio of 645.3 is negative 12, that at the  $m/z$  ratio of 704.6 is negative 11 and that at the  $m/z$  ratio of 774.9 is negative 10. When San was added, the species assigned

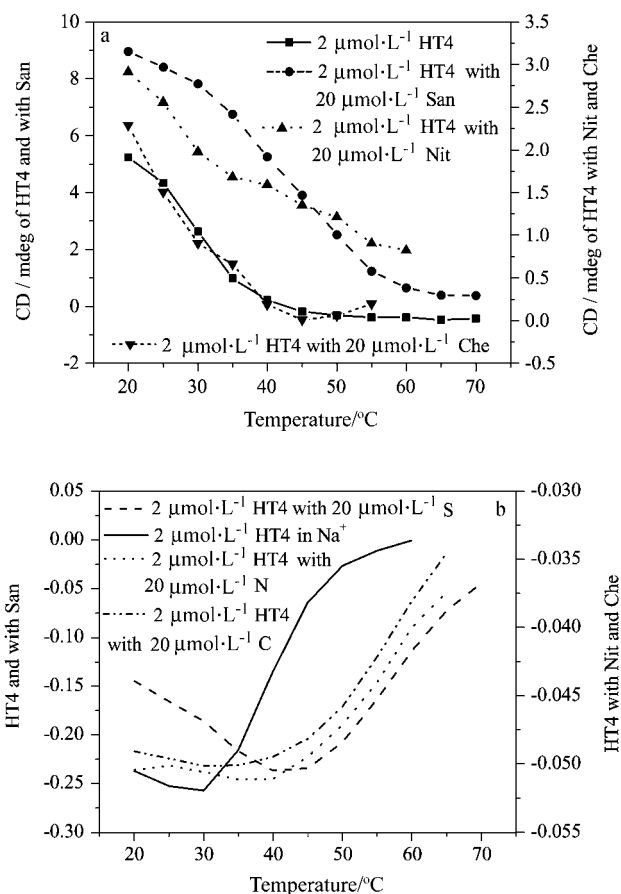


**Figure 4** (a) CD melting profiles of  $2 \mu\text{mol}\cdot\text{L}^{-1}$  HT4 G-quadruplex and  $2 \mu\text{mol}\cdot\text{L}^{-1}$  HT4 with  $20 \mu\text{mol}\cdot\text{L}^{-1}$  San, Nit and Che at 292 nm. (b) The second derivative curves of the changes of CD signals of  $2 \mu\text{mol}\cdot\text{L}^{-1}$  HT4 G-quadruplex and  $2 \mu\text{mol}\cdot\text{L}^{-1}$  HT4 with  $20 \mu\text{mol}\cdot\text{L}^{-1}$  San, Nit and Che at 292 nm against the temperature.

to HT4-San arrived at  $m/z$  ratio of 735.6 with the charge of negative 11 and the calculated molecular weight is just equal to the molecular weight of HT4 and San, suggesting that the G-quadruplex formed by San is intramolecular structure. In the case of Nit and Che, the same results could be obtained. All of these results suggest that QBAs induce single-strand HT4 to form intramolecular G-quadruplex structures.

### QBAs could induce human telomeric DNAs with different chain length forming G-quadruplex

To further investigate the QBAs' abilities to induce human telomeric DNA forming G-quadruplex, more experiments were performed on the inducing effects of QBAs on human telomeric DNA with different chain length. The results are summarized in Figure 6.

H7 is another human telomeric DNA with short chain, which can form only parallel intermolecular G-quadruplex structure under certain conditions.<sup>26</sup> Different from monovalent metal ion (such as  $\text{K}^+$ )<sup>26</sup> or some G-quadruplex ligands (such as RHPS4),<sup>27,28</sup> adding QBAs into H7 did not result in any significant

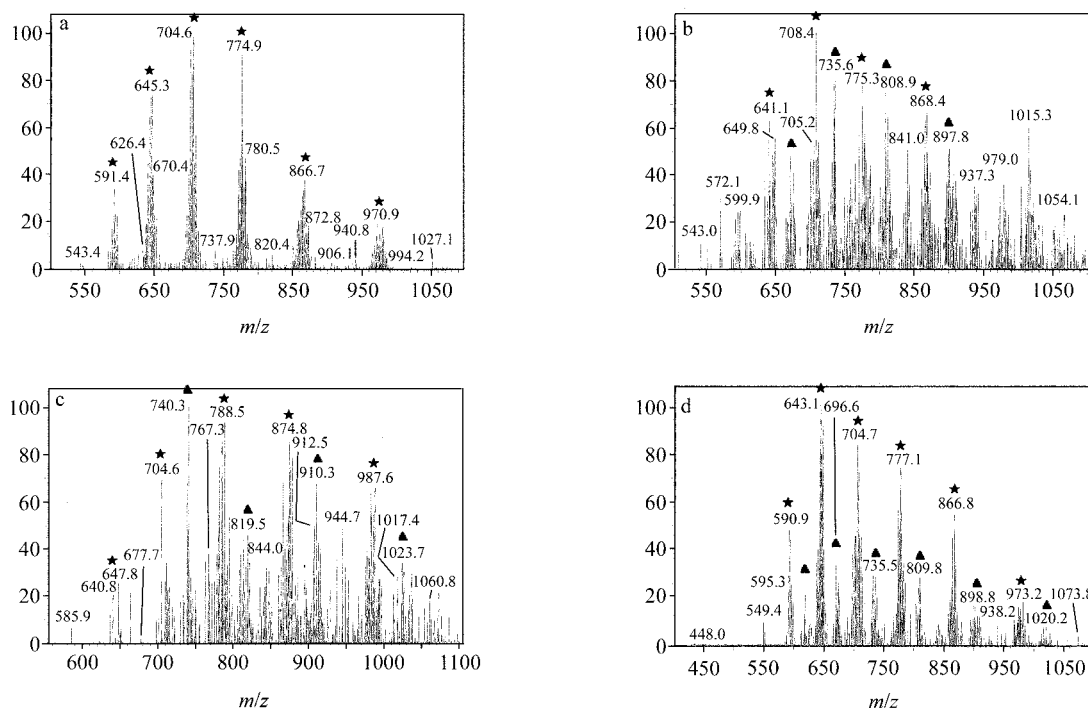


**Figure 5** The ESI spectra of  $6 \mu\text{mol}\cdot\text{L}^{-1}$  HT4 (a) and  $6 \mu\text{mol}\cdot\text{L}^{-1}$  HT4 with  $30 \mu\text{mol}\cdot\text{L}^{-1}$  San (b),  $30 \mu\text{mol}\cdot\text{L}^{-1}$  Nit (c) and  $60 \mu\text{mol}\cdot\text{L}^{-1}$  Che (d), respectively. The peaks signed by ★ are assigned to HT4 and the ones signed by ▲ are assigned to HT4-QBA complex.

changes of the CD spectra between 220 and 350 nm, indicating that QBAs could hardly induce H7 forming G-quadruplex structure.

In the case of HT2, it can form dimeric hairpin<sup>29</sup> or parallel intermolecular G-quadruplex structure<sup>30</sup> under certain conditions. As shown in Figure 6, the CD signals of HT2 were partially changed by adding San and Nit: the positive CD signal at 256.5 nm red shifts to 270 nm, most probably due to formation of parallel G-quadruplex structure.<sup>22</sup> However, Che red shifts the CD signal at 256.5 to 262 nm merely, less change observed than San and Nit, indicating weaker inducing ability.

For the longer chain telomeric DNA sequence, H22, H24A and HT4, they could form intramolecular but distinct G-quadruplex structures with metal ion. For example, H22 exist as parallel form with sodium,<sup>31</sup> H24A as hybrid form with potassium,<sup>32</sup> and HT4 as mixture of several different quadruplex forms with potassium.<sup>19,20,33,34</sup> As shown in Figure 6, the CD signals of H22, H24A and HT4 with random conformations have been dramatically changed. In the present of San and Che, the CD spectra exhibit typical feature of antiparallel G-quadruplex structure, while in the present of Nit, the CD spectra inferring the formation of mixed-type or hybrid G-quadruplex structure.

Generally, QBAs could induce sequences of human telomeric DNA with certain length forming G-quadruplex with varying degrees except H7 with short chain of only one (TTAGGG) residue. It is supposed that QBAs' selectivity for the chain length of DNAs is caused by their positive charges which could

not attract short chain DNA (such as H7) molecules to close to each other and form intermolecular G-quadruplex.

## Discussion

As mentioned previously, QBAs have a positively charged centre and extended  $\pi$ -aromatic plane. During the interaction between major ligands and the formed G-quadruplex, the positively charged centre may attract the G-quadruplex close-by, and then the aromatic rings would form face-to-face stacking on the G-quartets in the G-quadruplex structure, such as perylenetetracarboxylic diimide (PIPER),<sup>35</sup> berberine,<sup>36</sup> RHPS4,<sup>28</sup> etc.

The positive charged centre also acts as a "pseudo" potassium ion and is positioned above the centre of the G-quartets in the region of high negatively charged density. As far as the interaction between QBAs and single-strand HT4 is concerned, the positively charged centre in QBAs may play the same role. If the electrostatic interaction is the key factor responsible for the formation of different HT4 G-quadruplex structures induced by QBAs, the electrostatic distribution of the molecular frame should be different among three QBAs. Actually, the theoretical calculation on the electrostatic distributions of the structure-optimized QBAs (as shown in supporting information) have shown there is no distinct difference in the electrostatic distribution of the molecular frame among three QBAs, indicating electrostatic interaction may not be the key factor responsible for the formation of different HT4 G-quadruplex structures induced by QBAs.

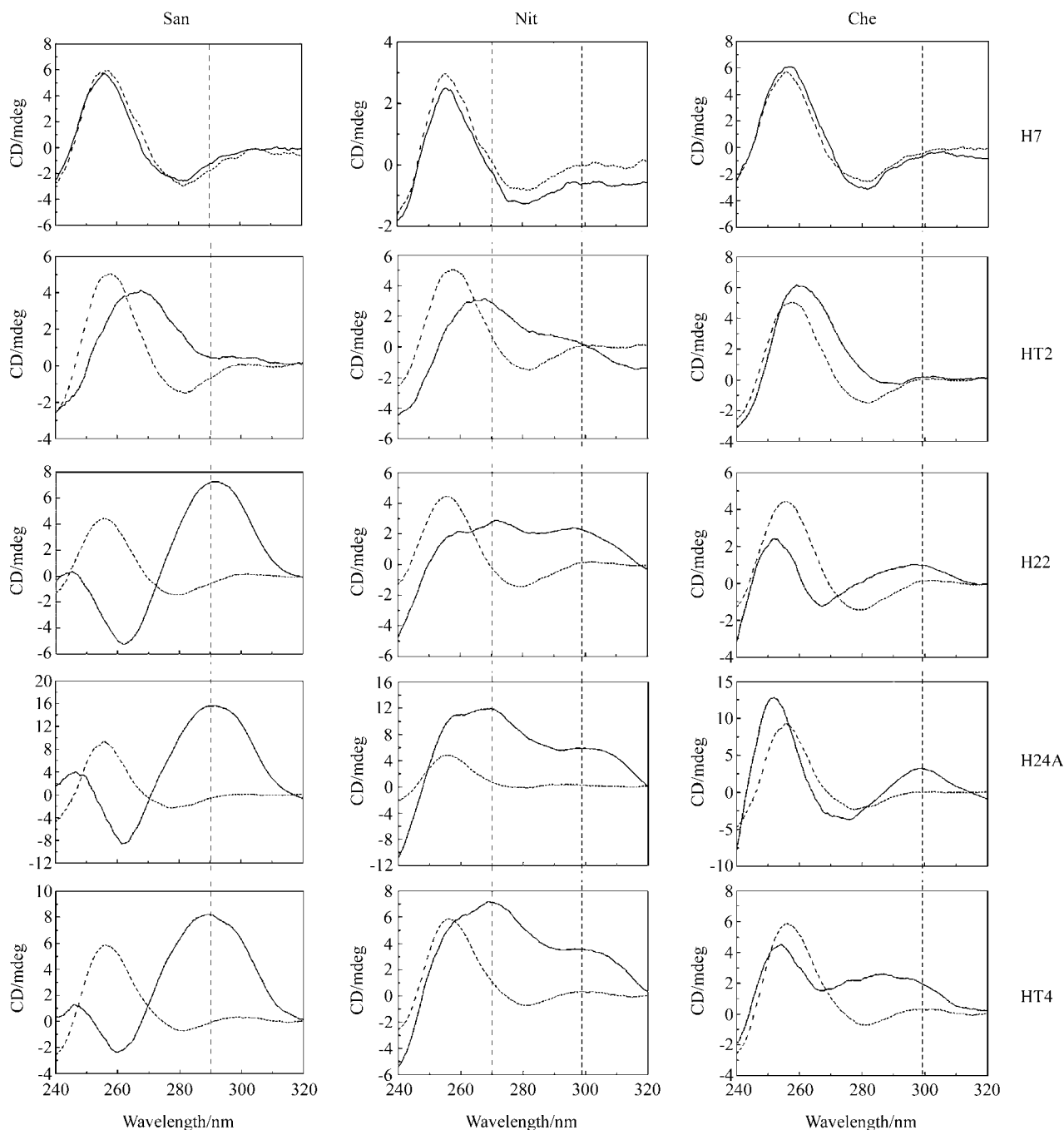


**Figure 6** The CD spectra of  $2 \mu\text{mol}\cdot\text{L}^{-1}$  various DNA sequences (dashed lines) and  $2 \mu\text{mol}\cdot\text{L}^{-1}$  various DNA sequences with  $10 \mu\text{mol}\cdot\text{L}^{-1}$  San, Nit and Che (solid lines), respectively.

On the other hand, as far as we know, ligands generally interact with G-quadruplex structure through intercalation, groove binding and end-stacking. The induced CD signals (ICD) could indicate the interaction mode because the molecular frame would be twisted and give rise to CD signals when the molecule bound to the G-quadruplex structure. It is reported that metalloporphyrins could give rise to strong positive ICD when bound to the groove of the G-quadruplex DNA<sup>37,38</sup> while free-base porphyrins with bulky substituents intercalating or end-stacking with the G-quadruplex

DNA only shows moderate ICD.<sup>39,40</sup> As shown in Figure 7, ICD of QBAs appeared at the wavelength range of 320–500 nm in the presence of HT4. One can see that during the formation of G-quadruplex structure, different ICD of QBAs appeared: a weak broad negative CD signal with  $\lambda_{\text{max}}$  at 350 nm for San, a weak broad positive CD band in the wavelength range of 350–450 nm for Nit, and no ICD for Che. Obviously, the relative weak ICD of QBAs was probably resulted from intercalation or end-stacking with HT4 G-quadruplex structures.

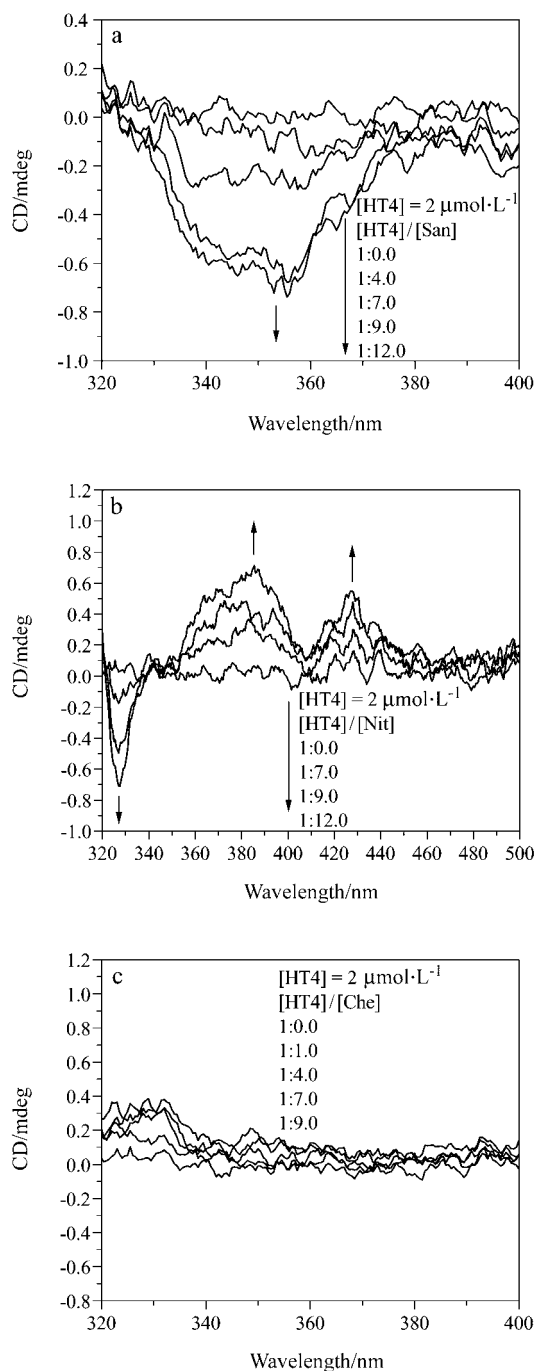


**Figure 7** The induced CD spectra of San (a), Nit (b) and Che (c) during the transformation of HT4 into G-quadruplex structures.

If QBA molecules intercalate within the induced HT4 G-quadruplex, the thickness of the molecular frame of QBAs may be a key factor. The interval of the G-quartets in integrated G-quadruplex structure has been reported *ac* 3.4 Å<sup>41</sup> and metal ions with diameter 1.3–1.5 Å<sup>42</sup> fit very well within the two G-quartets of quadruplex.<sup>43</sup> Obviously, the ring closure of two methoxyl groups makes San possess the thinnest thickness, which could facilitate maximum  $\pi$ - $\pi$  stacking between San and G-quartet rather than Nit and Che.

For Nit and Che, although the two methoxyl groups make both of them have no difference in the thickness,

they show different abilities in the interaction with HT4. Structurally, the difference of Nit and Che is merely the substituents at 9- and 11-position, so the steric hindrance at these sites is supposed to be another key factor responsible for the formation of different HT4 G-quadruplex structures induced by QBAs. This could be explained by the position of the positively charged centre, the quaternary ammonium at 7-position, which plays a very important role in attracting HT4. Compared with Che, Nit is substituted at the 11-position instead of 9-positions, indicating less steric hindrance close to the cationic core. Therefore, the thickness of D ring and the steric hindrance of the sensitive sites (the 9-, 10- and 11-substituents) are the reasons why the subtle differences in QBAs' structure lead to their remarkable differences in inducing the formation of the G-quadruplex structures.

## Conclusion

The interaction between human telomeric DNA (HT4) and three QBAs (San, Nit and Che) were discussed. Although these molecules are very similar in structure, they exhibit significantly different abilities in inducing single-strand DNA HT4 to specific G-quadruplex structures. Our experimental results indicated that the best ligand San could convert single-strand human telomeric DNA into antiparallel G-quadruplex structure completely, followed by Nit, which could transform to mixed-type or hybrid G-quadruplex structure partially, whereas Che could only transform to antiparallel G-quadruplex structure in small quantities. The relative QBAs' inducing abilities as indicated by the CD data are in the order of San > Nit > Che. And ESI results inferred that the G-quadruplex structures from HT4 induced by QBAs are of intramolecular motif. In addition, several DNA sequences derived from human telomeres were investigated and it is shown that only sequences with certain length could be induced to form G-quadruplex structure by QBAs. It is supposed that QBAs' selectivity is caused by their positive charges which could not attract short chain DNA (such as H7) molecules to close to each other and form intermolecular G-quadruplex.

Furthermore, the factors affecting the interaction between HT4 and QBAs are discussed. It is proposed that the thickness of the molecular frame and the steric hindrance of the substituents at 9-, 10-, and 11-position of QBAs are the key factors.

This observation, together with the previous reports concerned with the interaction with duplex-strand DNA<sup>15</sup> and G-quadruplex,<sup>18</sup> has suggested that the slightly structural difference can bring to large difference in the properties. Thus careful examination of the structural effect of G-quadruplex ligands on their properties is necessary in further finding and designing efficient antitumor agents.



## Supporting Information

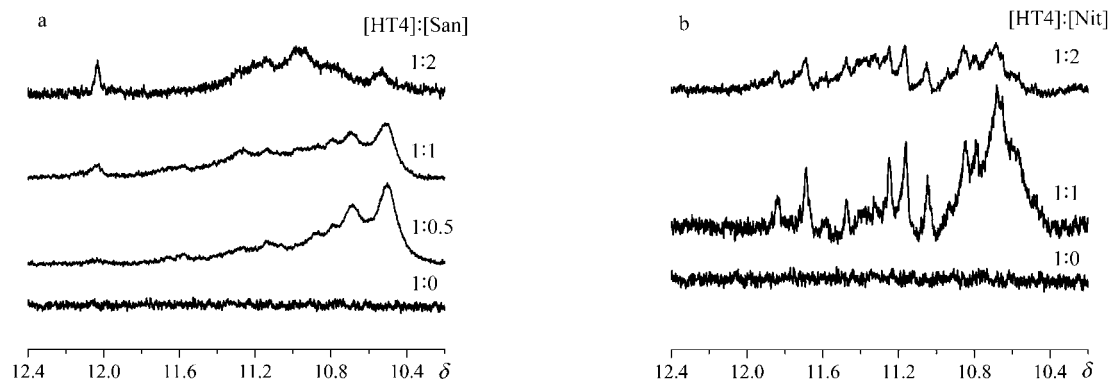


**Figure S1**  $^1\text{D}$  NMR spectra of 80  $\mu\text{mol}\cdot\text{L}^{-1}$  HT4 and 80  $\mu\text{mol}\cdot\text{L}^{-1}$  HT4 with San (a) and Nit (b).

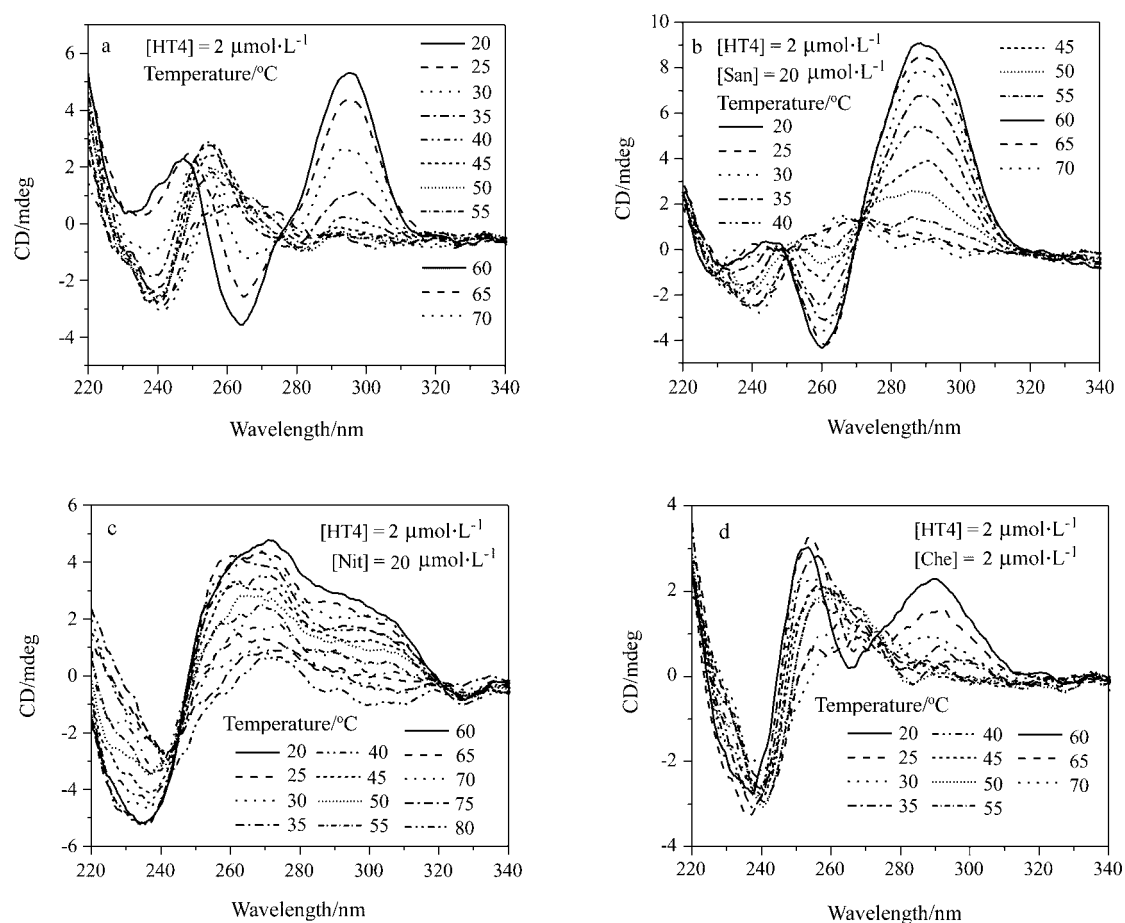


**Figure S2** CD spectra of 2  $\mu\text{mol}\cdot\text{L}^{-1}$  HT4 (a) and 2  $\mu\text{mol}\cdot\text{L}^{-1}$  HT4 with 20  $\mu\text{mol}\cdot\text{L}^{-1}$  San (b), Nit (c) and Che (d) under different temperatures.

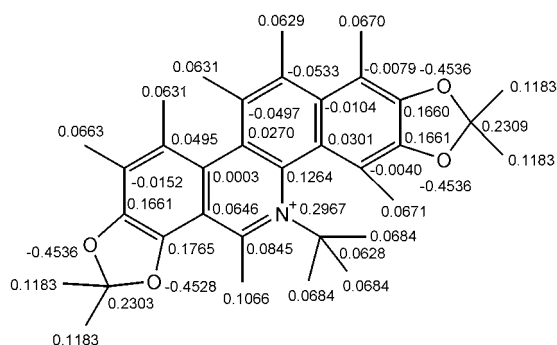


**Figure S3** Graphics of theoretical electrostatic distributions of the structure-optimized San.

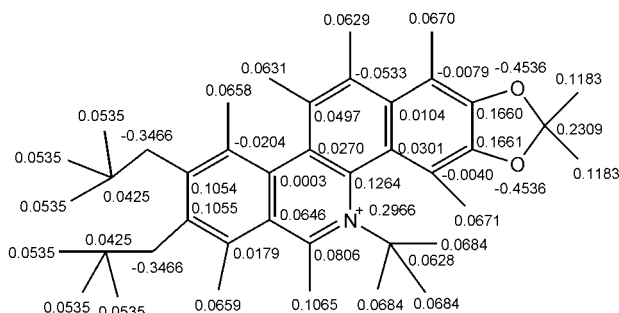


**Figure S4** Graphics of theoretical electrostatic distributions of the structure-optimized Nit.

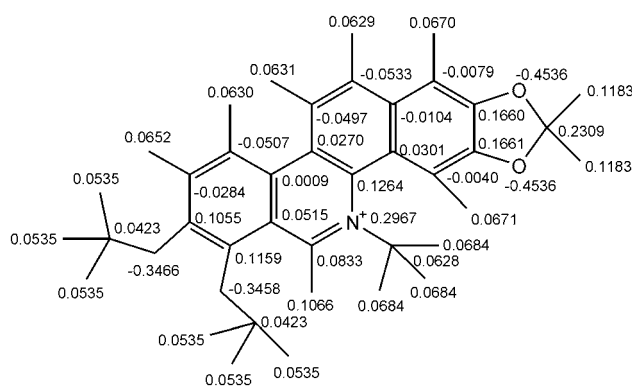


**Figure S5** Graphics of theoretical electrostatic distributions of the structure-optimized Che.

## References

- 1 De Cian, A.; Lacroix, L.; Douarre, C.; Temime-Smaali, N.;  
Trentesaux, C.; Riou, J. F.; Mergny, J. L. *Biochimie* **2008**,  
90, 131.
- 2 Blackburn, E. H. *Cell* **2001**, 106, 661.
- 3 Kim, N. W.; Piatuszek, M. A.; Prowse, K. R.; Harley, C. B.;  
West, M. D.; Ho, P. L.; Coviello, G. M.; Wright, W. E.;  
Weinrich, S. L.; Shay, J. W. *Science* **1994**, 266, 2011.
- 4 Davis, J. T. *Angew. Chem., Int. Ed.* **2004**, 43, 668.
- 5 Zahler, A. M.; Williamson, J. R.; Cech, T. R.; Prescott, D. M.  
*Nature* **1991**, 350, 718.
- 6 Ou, T. M.; Lu, Y. J.; Tan, J. H.; Huang, Z. S.; Wong, K. Y.;  
Gu, L. Q. *ChemMedChem* **2008**, 3, 690.

- 7 Monchaud, D.; Teulade-Fichou, M. P. *Org. Biomol. Chem.* **2008**, *6*, 627.
- 8 Zhou, Q.; Li, L.; Xiang, J.; Tang, Y.; Zhang, H.; Yang, S.; Li, Q.; Yang, Q.; Xu, G. *Angew. Chem., Int. Ed.* **2008**, *47*, 5590.
- 9 Sun, H.; Xiang, J.; Tang, Y.; Xu, G. *Biochem. Biophys. Res. Commun.* **2007**, *352*, 942.
- 10 Goncalves, D. P. N.; Rodriguez, R.; Balasubramanian, S.; Sanders, J. K. M. *Chem. Commun.* **2006**, 4685.
- 11 Prado, S.; Michel, S.; Tillequin, F.; Koch, M.; Pfeiffer, B.; Pierre, A.; Leonce, S.; Colson, P.; Baldeyrou, B.; Lansiaux, A.; Bailly, C. *Bioorg. Med. Chem.* **2004**, *12*, 3943.
- 12 Cabrespine, A.; Bay, J. O.; Barthomeuf, C.; Cure, H.; Chollet, P.; Debiton, E. *Anti-Cancer Drugs* **2005**, *16*, 417.
- 13 Chmura, S. J.; Dolan, M. E.; Cha, A.; Mauceri, H. J.; Kufe, D. W.; Weichselbaum, R. R. *Clin. Cancer Res.* **2000**, *6*, 737.
- 14 Maiti, M.; Kumar, G. S. *Med. Res. Rev.* **2007**, *27*, 649.
- 15 Bai, L. P.; Zhao, Z. Z.; Cai, Z.; Jiang, Z. H. *Bioorg. Med. Chem.* **2006**, *14*, 5439.
- 16 Read, M.; Harrison, R. J.; Romagnoli, B.; Tanious, F. A.; Gowan, S. H.; Reszka, A. P.; Wilson, W. D.; Kelland, L. R.; Neidle, S. *Proc. Natl. Acad. Sci. U. S. A.* **2001**, *98*, 4844.
- 17 Reed, J. E.; Arnal, A. A.; Neidle, S.; Vilar, R. *J. Am. Chem. Soc.* **2006**, *128*, 5992.
- 18 Bai, L. P.; Hagihara, M.; Jiang, Z. H.; Nakatani, K. *Chem-BioChem* **2008**, *9*, 2583.
- 19 Li, J.; Correia, J. J.; Wang, L.; Trent, J. O.; Chaires, J. B. *Nucleic Acids Res.* **2005**, *33*, 4649.
- 20 Rujan, I. N.; Meleney, J. C.; Bolton, P. H. *Nucleic Acids Res.* **2005**, *33*, 2022.
- 21 Ambrus, A.; Chen, D.; Dai, J.; Bialis, T.; Jones, R. A.; Yang, D. *Nucleic Acids Res.* **2006**, *34*, 2723.
- 22 Balagurumoorthy, P.; Brahmachari, S. K. *J. Biol. Chem.* **1994**, *269*, 21858.
- 23 Bean, R. C.; Shepherd, W. C.; Kay, R. E.; Walwick, E. R. *J. Phys. Chem.* **1965**, *69*, 4368.
- 24 Zhou, J.; Yuan, G.; Liu, J.; Zhan, C. G. *Chem.-Eur. J.* **2007**, *13*, 945.
- 25 Li, W.; Zhang, M.; Zhang, J. L.; Li, H. Q.; Zhang, X. C.; Sun, Q.; Qiu, C. M. *FEBS Lett.* **2006**, *580*, 4905.
- 26 Wang, Y.; Patel, D. J. *Biochemistry* **1992**, *31*, 8112.
- 27 Gavathiotis, E.; Heald, R. A.; Stevens, M. F.; Searle, M. S. *J. Mol. Biol.* **2003**, *334*, 25.
- 28 Gavathiotis, E.; Heald, R. A.; Stevens, M. F.; Searle, M. S. *Angew. Chem., Int. Ed.* **2001**, *40*, 4749.
- 29 Keniry, M. A.; Strahan, G. D.; Owen, E. A.; Shafer, R. H. *Eur. J. Biochem.* **1995**, *233*, 631.
- 30 Parkinson, G. N.; Lee, M. P.; Neidle, S. *Nature* **2002**, *417*, 876.
- 31 Wang, Y.; Patel, D. J. *Structure* **1993**, *1*, 263.
- 32 Luu, K. N.; Phan, A. T.; Kuryavyi, V.; Lacroix, L.; Patel, D. J. *J. Am. Chem. Soc.* **2006**, *128*, 9963.
- 33 Granotier, C.; Pennarun, G.; Riou, L.; Hoffschir, F.; Gauthier, L. R.; De Cian, A.; Gomez, D.; Mandine, E.; Riou, J. F.; Mergny, J. L.; Mailliet, P.; Dutrillaux, B.; Boussin, F. D. *Nucleic Acids Res.* **2005**, *33*, 4182.
- 34 Phan, A. T.; Luu, K. N.; Patel, D. J. *Nucleic Acids Res.* **2006**, *34*, 5715.
- 35 Fedoroff, O. Y.; Salazar, M.; Han, H.; Chemeris, V. V.

- Kerwin, S. M.; Hurley, L. H. *Biochemistry* **1998**, *37*, 12367.
- 36 Zhou, J. L.; Lu, Y. J.; Ou, T. M.; Zhou, J. M.; Huang, Z. S.; Zhu, X. F.; Du, C. J.; Bu, X. Z.; Ma, L.; Gu, L. Q.; Li, Y. M.; Chan, A. S. *J. Med. Chem.* **2005**, *48*, 7315.
- 37 Ward, B.; Skorobogaty, A.; Dabrowiak, J. C. *Biochemistry* **1986**, *25*, 7827.
- 38 Lubitz, I.; Borovok, N.; Kotlyar, A. *Biochemistry* **2007**, *46*, 12925.
- 39 Kuhlmann, K. F.; Charbeneau, N. J.; Mosher, C. W. *Nucleic Acids Res.* **1978**, *5*, 2629.
- 40 Sehlstedt, U.; Kim, S. K.; Carter, P.; Goodisman, J.; Vollano, J. F.; Norden, B.; Dabrowiak, J. C. *Biochemistry* **1994**, *33*, 417.
- 41 Forman, S. L.; Fetting, J. C.; Pieraccini, S.; Gottarelli, G.; Davis, J. T. *J. Am. Chem. Soc.* **2000**, *122*, 4060.
- 42 Novy, J. *Biopolymers* **2007**, *89*, 144.
- 43 Kankia, B. I.; Marky, L. A. *J. Am. Chem. Soc.* **2001**, *123*, 10799.

(E0909181 Ding, W.; Fan, Y.)